FAST LOCAL BUMP SYSTEM FOR HELICITY SWITCHING AT THE PHOTON FACTORY

S. Matsuba*, Hiroshima University, Higashi-Hiroshima, Japan
K. Harada, Y. Kobayashi, T. Miyajima, S. Nagahashi, T. Obina, KEK, Ibaraki, Japan.

Abstract

In a south straight section of the Photon Factory storage ring (PF-ring), tandem APPLE-II type variably polarizing undulators will be installed with five fast bump kicker magnets in order to generate a local orbit bump for the helicity switching at a frequency of 10 Hz. At present, the installation of one undulator and a fast orbit bump system were completed and the machine studies to produce an orbit switching are in progress. In this paper, we describe an overview of the system, and the principal parameters of the bump magnets. In addition, we present the magnetic field measurements, the installation, and the preliminary results of the machine studies.

INTRODUCTION

In order to pick up the weak signals for measuring the photon polarization dependence of the materials [1], fast helicity switching of the undulator radiation with lock-in detection [2] is one of the excellent methods. Tandem APPLE-II type undulators with five fast orbit bump system will be installed in a south long straight section to realize the helicity switching. The undulators with alternate helicities are aligned on the straight line. The local angular orbit bump allows us to switch the photons delivered to the user beam line. Using the lock-in technique, a switching frequency of at least 10 Hz is required. Moreover, an angular bump of 0.3 mrad is also required for the separation of the photons generated from two undulators. The conceptual design overview is shown in Fig. 1. During spring shutdown in 2008, first undulator together with a bump system was installed into the ring.

OVERVIEW OF THE SYSTEM

For the orbit switching, five bump kicker magnets with an identical power supply are adopted. To realize the angular bump of 0.3 mrad in the undulator, the maximum kick angle of 2.4 mrad was required from the geometrical configuration. The principal parameters are listed in Table 1 and the cross sectional view of the magnetic core is shown in Fig. 2. Two-dimensional magnetic field is calculated by POISSON code [3].

Fast beam position monitor (BPM) is required to measure an orbit oscillation with a frequency of more than 10 Hz [4]. Three BPMs are located inside the bump and the other two are located outside the bump as shown in Fig. 3. To correct the orbit leakages due to the magnetic errors and the effects of the undulators, four fast steering magnets are installed. When the undulator has a skew quadrupole field component, a vertical orbit leakage is generated with the horizontal bump. Static skew quadrupole magnet enables us to easily correct such orbit leakage. Thus, free space for two skew quadrupole magnets for future installation are prepared for the correction of the vertical orbit.

MAGNETIC FIELD MEASUREMENT

Before we installed the bump system into the PF-ring, we measured the magnetic field distribution, the excitation curve and the frequency response. The hall probe (F.W.Bell 9500A) was used for the field measurement and the FFT analyzer (HP 3562A) for the

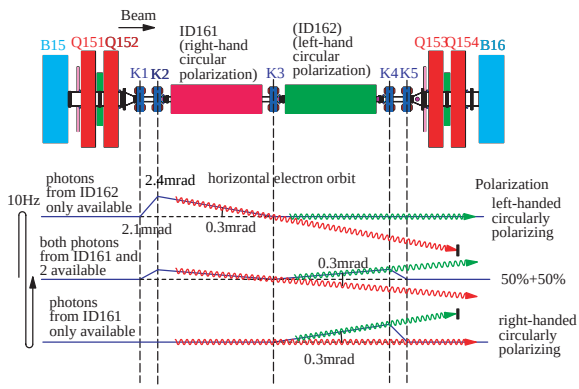

Figure 1: Schematic drawing of the conceptual design for producing the fast helicity switching variable polarized photon.

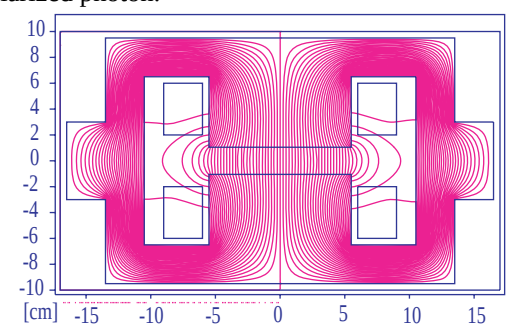

Figure 2: Cross sectional view of the bump kicker magnet. The magnetic field is calculated by two-dimensional POISSON code.

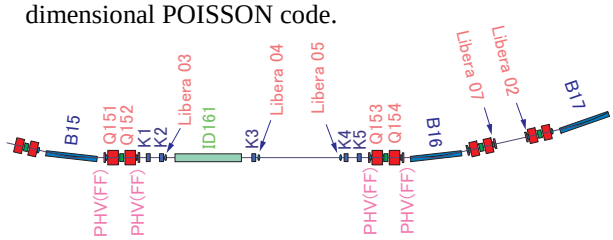

Figure 3: Schematic drawing of the system along the PF-ring lattice configuration. Labels of K1~K5, Libera, and PHV represent bump kicker magnets, fast BPMs and fast correction magnets in both of horizontal and vertical directions, respectively.

*shunya@post.kek.jp

Table 1: Principal parameters of the system

Max. beam energy	E [GeV]	3
Max. kick angle	θ [mrad]	2.4
Max. magnetic field (3GeV)	B [T]	0.16
Vertical pole gap	h [mm]	21
Horizontal pole width	w [mm]	110
Magnet core length	l [mm]	150
Coil turn number	N [turns]	32
Inductance	L [H]	1.0×10^{-3}
Maximum magnetic current (3GeV)	I [A]	83.5
Resistance	R [Ω]	0.1
Design bump frequency	f [Hz]	10
Max. voltage for 10Hz operation	V [V]	13.7
Silicon steel thickness	t [mm]	0.5
Power supply capacity	I [A]	±100
	V [V]	±50

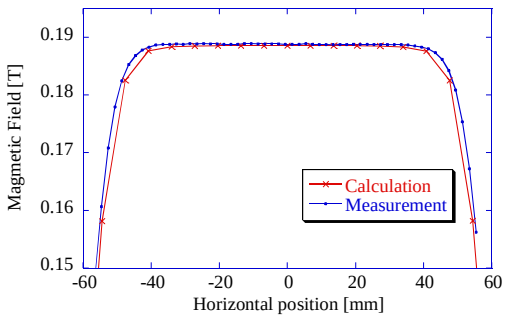

Figure 4: Typical horizontal distribution of the magnetic field. Solid blue line and red crosses show the results of the measurement and the calculation, respectively.

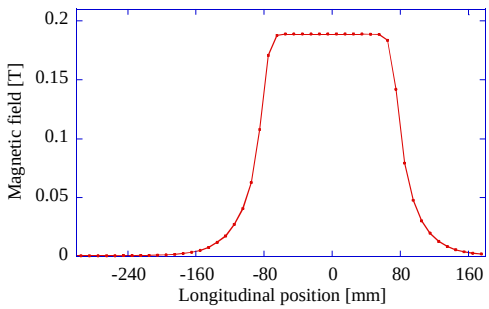

Figure 5: Typical longitudinal field distribution of the magnetic field.

frequency response measurement. The measurements were carried out for all five magnets. As a result, the individual differences were less than 1×10^{-3}. Figure 4 shows a typical horizontal field distribution. The measured results agreed well with the results calculated by the POISSON code. The flatness of the magnetic field ($\Delta B/B$) was smaller than 1×10^{-3} in $|x| < \pm 35$ mm. Fig. 5 shows typical longitudinal (beam direction) field distribution. The measured region was limited by the capacity of the movable stage where the hall probe was

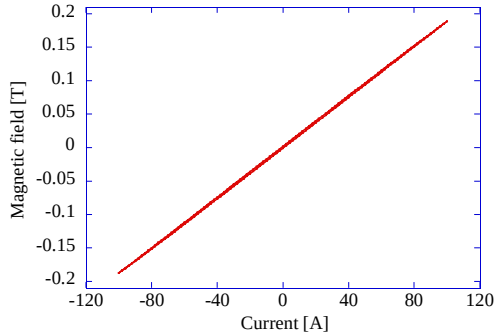

Figure 6: Typical excitation curve of the magnetic field.

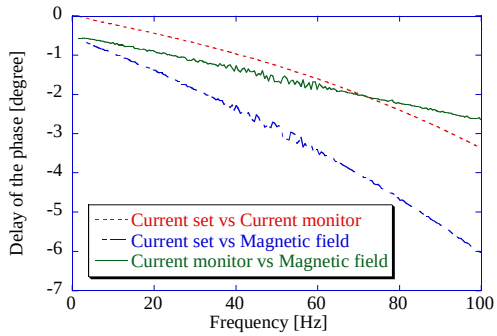

Figure 7: Typical phase delay as a function of the switching frequency. Three lines represent the phase delay: (red) between input signal and output current, (blue) between input signal and magnetic field, and (green) between output current and magnetic field.

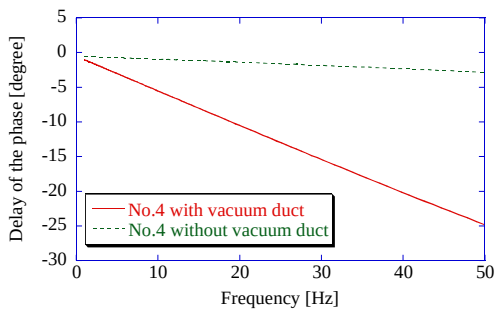

Figure 8: Typical phase delay as a function of switching frequency. Two lines represent the phase delay: (red) with a vacuum duct and (green) without a vacuum duct.

attached. The magnetic core was located at $|z| < \pm 75$ mm. The fringing field was reasonable and the effective length was estimated to be 183 mm. Figure 6 shows a typical excitation curve measured by the hall probe. Due to the hysteresis effect, the residual magnetic field was about 0.0015 T which corresponds to the kick angle of 0.02 mrad for the beam energy of 2.5GeV. In order to suppress the leakage of the local bump to avoid the disturbance for the users at the other beam lines, it is essential to suppress the hysteresis effect by preserving the constant current loop and to correct the orbit distortion.

Figure 7 shows a typical phase delay without a vacuum duct in the frequency response measurement. At the

frequency of 10 Hz, the phase delay of 0.2 deg to the input control signal was produced in the output current of the power supply. For the excitation of the magnetic field the delay to the output current was 0.7 deg Figure 8 shows same as the Fig. 7, but the phase delay with and without a vacuum chamber. The phase delay increased from 0.7 deg to 5.5 deg at a frequency of 10 Hz. Therefore, it is also essential to compensate the phase delay.

INSTALLATION TO THE PF RING

During spring shutdown in 2008, previous multipole wiggler of MPW16 was removed from a south long straight section and new undulator, U161, was installed in an upstream part of the same section with the bump system. For the alignment of the magnets, a levelling scope (Wild N3), a transit (Kern T3000), a metal ruler and a water level were employed. The tolerances of the alignment errors were ±100 μm for both of the horizontal and vertical directions, and ±500 μm for the longitudinal direction. Since the magnetic field of the bending magnet is almost constant near the beam axis, tolerances of the parallel shift are not so severe. On the other hand, with the rotation error, the horizontal kick generates vertical orbit distortion. The tolerance of the rotation error was ±0.2 mrad. We confirmed that the tolerances were within our goal values by the re-survey after the fine alignments.

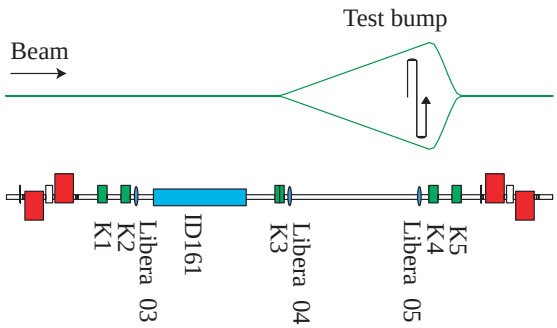

Figure 9: Schematic drawing of the angular bump produced by three kicker magnets of K3, K4 and K5 with the lattice configuration around the system. The bump was sinusoidally switched, indicated by the black arrow.

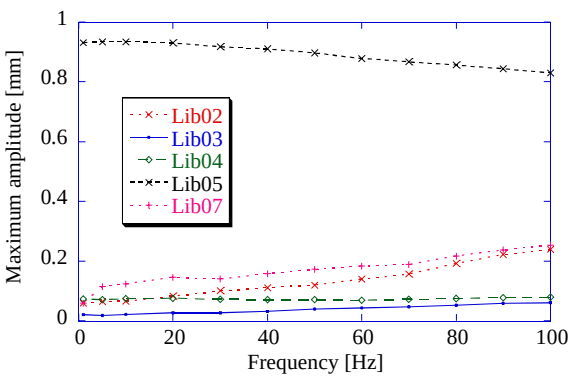

Figure 10: Horizontal oscillation amplitude as a function of the switching frequency detected using five fast BPMs. Black crosses (Lib05) and open circles (Lib04) represent the amplitudes inside the test bump, and the others outside the bump.

RESULTS OF PRELIMINARY MACHINE STUDY

After the commissioning of the ring and new undulator, the machine studies to generate the local bump were conducted. The bipolar sinusoidal bump for the undulator as shown in Fig. 9 was firstly produced in order to check the performance of the system. When the ideal bump has maximum amplitude without error, the measured bump height would be 0.057 mm at “Libera 04”, 0.99 mm at “Libera 05” and zero for other BPMs for the test bump with K3, K4 and K5 for the straight section without undulator.

Fig. 10 shows the measured amplitude of the fast BPMs. In this measurement, the bump was sinusoidal and the peak magnetic currents were I_{K3} = 7.51 A, I_{K4} = –58.49 A, and I_{K5} = 51.73 A. When the switching frequency was larger than 20 Hz, the difference of the phase delay for each magnet was increased as a function of the frequency. At the 0.1 Hz operation, the horizontal beam amplitude outside of the bump is about ±10 μm at the maximum and the vertical one about ±5 μm.

CONCLUSION

One APPLE-II type variably polarizing undulator with a fast local bump system for the helicity switching was installed into a south long straight section. Before we installed the bump system, we measured the magnetic field distribution, the excitation curve and the frequency response. After the installation, the machine studies were carried out. Through the hardware check of the magnets and the power supplies in the studies we confirmed that the bump system satisfied the design performance.

ACKNOWLEDGEMENT

The authors would like to gratefully acknowledge Mr. Y. Ohsawa and Prof. M. Masuzawa for the kind instructions, advices and great help for the alignment of the bump kicker magnets.

REFERENCES

[1] G. Schutz et al., Phys. Rev. Lett. 58, (1987) 737
[2] T. Hara et al., “Helicity switching of circularly polarlized undulator radiation by local orbit bumps”, NIM A, 498 (2003) pp496-502
[3] POISSON/SUPERFISH, Los Alamos National Laboratory Report, LA-UR-96-1834.
[4] Libera family beam diagnostic instruments, http://www.i-tech.si/